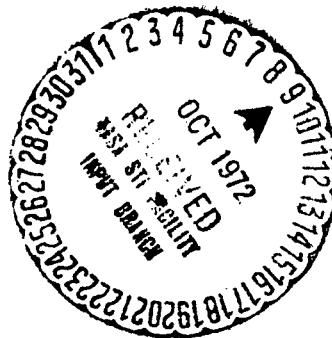


FLOW CONTROL BY CROSS JET

H. Werlé and M. Gallon

Translation of: "Contrôle d'écoulements par  
jet transversal," L'Aéronautique et l'Astro-  
nautique, No. 34, 1972, pp. 21-33.

(NASA-TT-F-14548) FLOW CONTROL BY CROSS N72-32303  
JET H. Werle, et al (Scientific  
Translation Service) Sep. 1972 23 p CSCL  
20D Unclas  
G3/12 41815



Details of illustrations in  
this document may be better  
seen in microfilm

NATIONAL AERONAUTICS AND SPACE ADMINISTRATION  
WASHINGTON, D. C. 20546 SEPTEMBER 1972

Reproduced by  
NATIONAL TECHNICAL  
INFORMATION SERVICE  
U S Department of Commerce  
Springfield VA 22151

## FLOW CONTROL BY CROSS JET

Henri Werlé and Marc Gallon

ABSTRACT. Studies carried out by the Lockheed Company and by ONERA showed that a jet oriented crosswise reduces noticeably the flow separation around models.

Water tunnel visualizations presented in this article confirm results obtained in air. They show, in particular, the flow pattern and its evolution through the jet action, and reveal the process efficiency in a variety of cases: cylinder, perpendicular flat plate, contoured wall, rearward step, unswept wing, deflected flap, swept wing, diverging duct, fluidic system, etc.

### Introduction

/21\*

As a means of reducing flow separation over a wing, the cross-jet method was proposed for the first time by C.J. Dixon [1], who applied it to a very thin unswept wing with aspect ratio  $\lambda = 4.4$ .

In point of fact, this type of flow control is part of the lateral stream system whose effectiveness was demonstrated at ONERA as early as 1960 [2] during tests on a cylinder and a flat plate mounted perpendicular to the air stream. Indeed, the visualizations obtained at this time (Figure 1) showed that the wakes of these two models could be reduced to two symmetric, steady vortices under the action of lateral currents induced by two jets associated with two ducts (see the mounting diagram of Figure 1A). We find that the wake which results from the confluence of the separations over the various parts of the models is resorbed more for the cylinder (the points of separation are closer together: Figures 1B and 1C) than for the perpendicular plate (separation fixed along the sharp edges of the model: Figures 1D and 1E).

---

\* Numbers in the margin indicate pagination in the original foreign text.

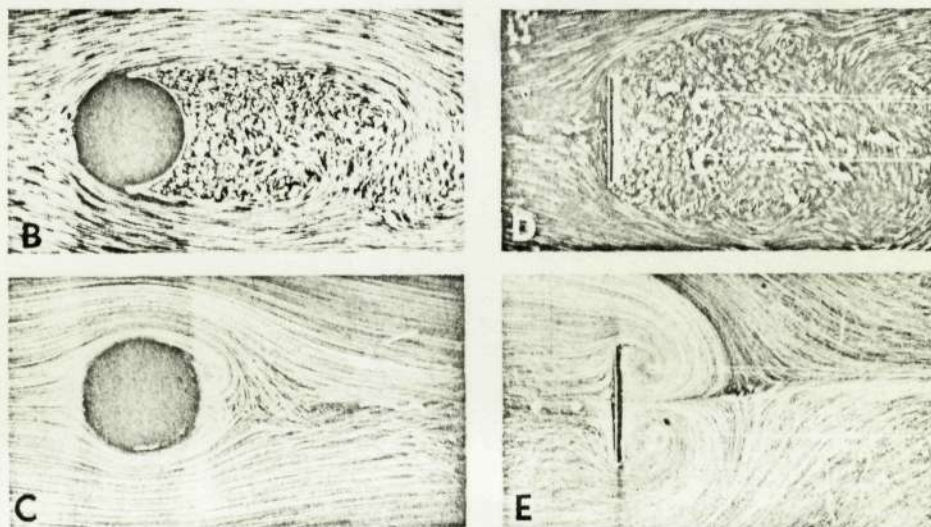
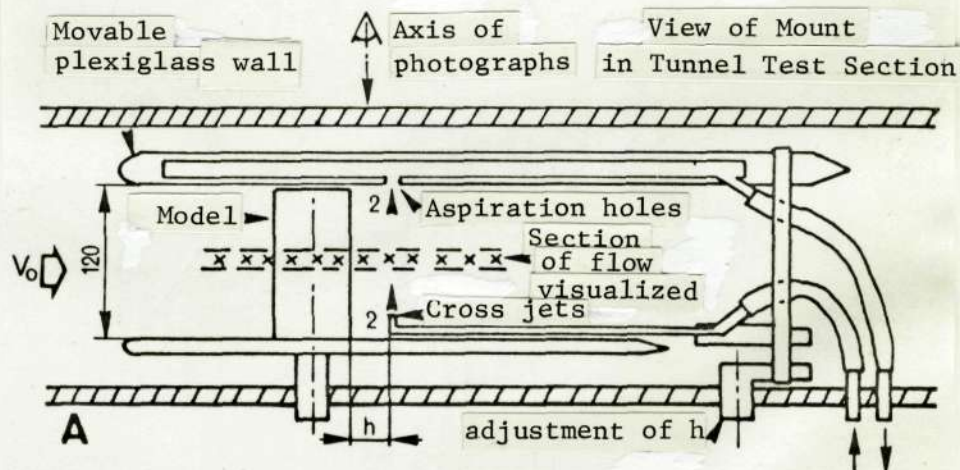


Figure 1. Control of flow around a "plane stream" model by two lateral jets issuing into the wake.

A Diagram of mounting

B Cylinder without jet

C Cylinder with jets

D Perpendicular plate without jet

E Perpendicular plate with jets

$$d = 40 - Re_d \simeq 2 \times 10^3$$

Visualizations by  
air bubbles

$$l = 40 - Re_l \simeq 10^3 - i = 90^\circ$$

The importance of these lateral currents on the flow around models has been emphasized since 1957 by M. Roy [3], who inspired these studies.

Later, other hydrodynamic-tunnel tests showed that a jet of the same type would retard the appearance of bursting phenomena which disrupts the apex vortices of a delta wing at large angles of attack [4]: see Figures 8A and 8B.

Finally, more recently, these different studies have been repeated and other applications of lateral blowing have been studied by Lockheed [5] and by ONERA, where they were the object of a series of tests in the wind tunnel at the Cannes center, as well as in the hydrodynamic tunnel at Chatillon [6] and [7]. /22

The present paper, announced in "L'Aeronautique et l'Astronautique," No. 22 [8], is limited for the most part to results obtained by this latter method.

### Experimental Technique

The visualizations which illustrate this paper were made in the normal test section (22 cm by 22 cm) of the hydrodynamic tunnel, in which the maximum velocity barely exceeds 20 cm/s. Under these conditions, the Reynolds number achieved amounts to 2000 per cm of model, which confers a generally qualitative character to the results obtained.

The interested reader will find in [9] or [10] the characteristics of the tunnel, the mounts, and the methods used for many years, whose range of application has recently been extended to transient flows [11].

Let us merely remark that the visualization was produced by minute air bubbles suspended in the water (e.g., Figures 1, 2, 3C, 3E, etc.) or by injection of colored liquids of unit density (e.g., Figures 3B, 3D, 5C, etc.). /23

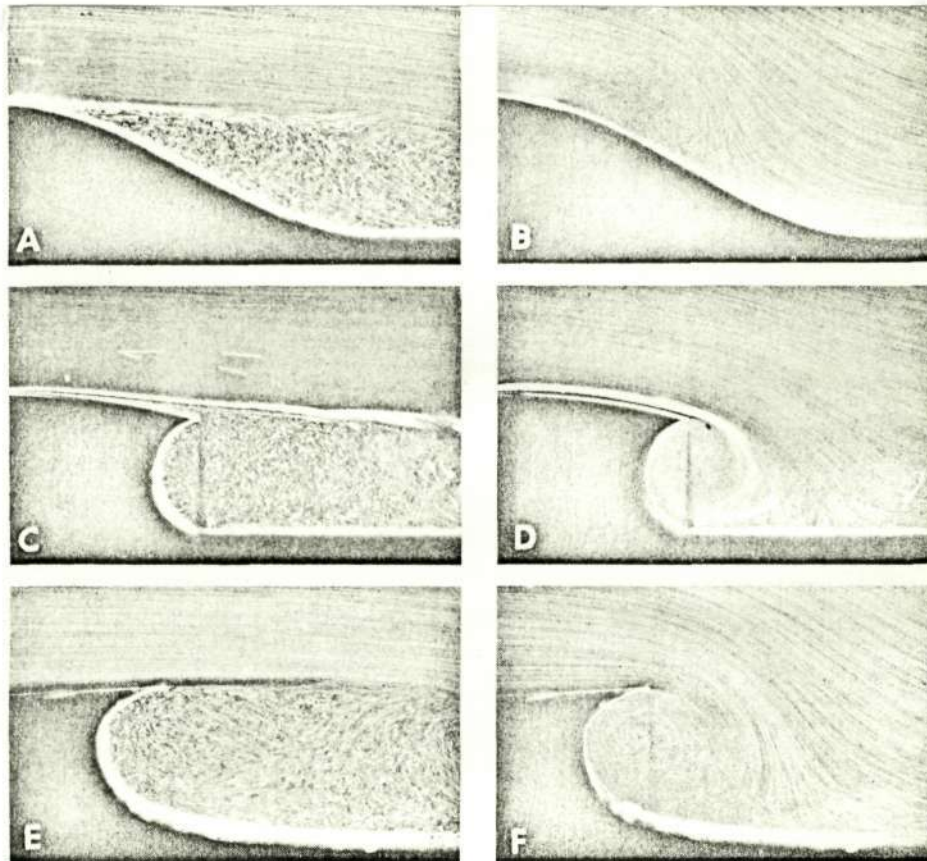


Figure 2. Cross-jet control of flow along a wall with an inward curve or a pronounced step ("plane stream" models).

- |   |                         |   |                                      |
|---|-------------------------|---|--------------------------------------|
| A | Curved wall without jet | } | continuous model (no point)          |
| B | Curved wall with jet    |   |                                      |
| C | Step wall without jet   | } | model with point sloping toward wall |
| D | Step wall with jet      |   |                                      |
| E | Step wall without jet   | } | model with point sloping outward     |
| F | Step wall with jet      |   |                                      |

Visualizations by air bubbles  $Re \simeq 2 \times 10^4$

### Fundamental Experiments

The reduction of the wake from a zero-circulation, "plane stream" model to two symmetric vortices was mentioned above (Figure 1). A second basic case



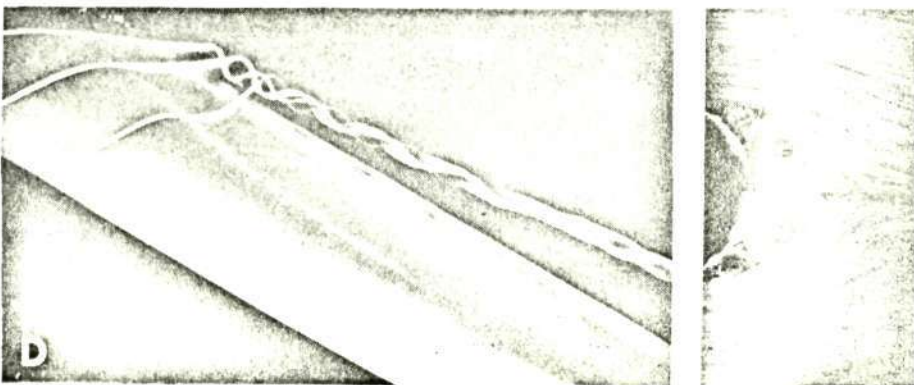
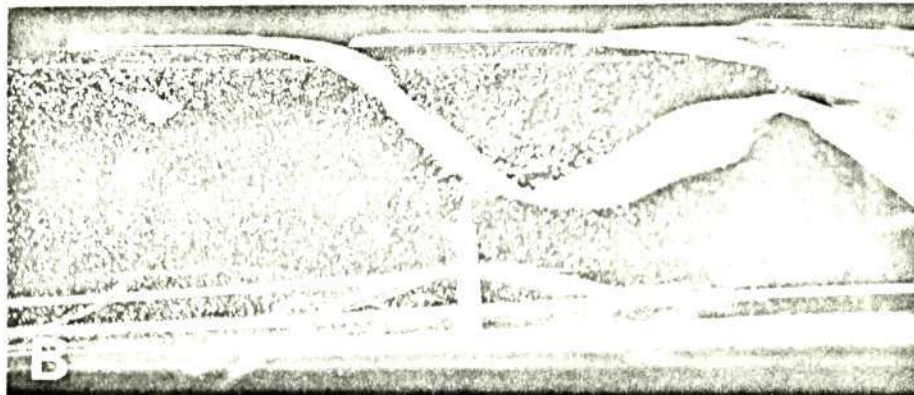
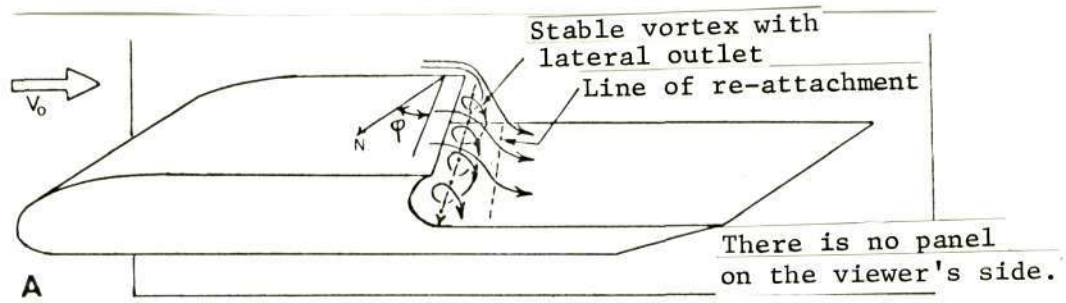


Figure 3 . Caption on following page.

Figure 3. (Continued) Control of flow around a strongly-swept model by natural cross current.

A	Diagram of flow	} Wall with strongly swept re-entrant ( $\varphi=60^\circ$ ) $Re \simeq 2 \cdot 10^4$
B	Flow in the re-entrant step	
C	Longitudinal section of flow	
D	Flow behind the model, plan view	} Swept cylinder ( $\varphi=60^\circ$ ) $d=40 - Re_d \simeq 0,4 \cdot 10^4$
E	Transverse view, normal to generators	
B and D visualization by colored liquid.		
C and E visualization by air bubbles.		

is that of separation on an asymmetric "plane stream" model, such as occurs on a wall with a strong curvature (Figure 2A) or a large re-entrant step (Figures 2C and 2E). In the absence of any jet effect, a more or less extensive separated region forms on these models. The upstream portion consists of still water which does not exchange with the laminar external flow; the downstream portion contains a zone of more turbulent mixing.

As in the symmetric case, a cross jet in the still water reduces the separation to a closed turbulent zone more or less centered around the jet.

On the wall which is curved inward, but continuous (Figure 2B), a small separation remains ahead of the obstacle formed by the jet, while downstream the flow re-attaches behind the turbulent jet, and immediately becomes laminar again.

In contrast, the more or less circular cavity, which characterizes the re-entrant steps studied (Figures 2d and 2F), is best adapted to the presence of a cross jet. Thus, the jet turns in the cavity and absorbs the low-energy boundary layer without making it separate upstream. The external flow passes around this fluid hinge and reattaches downstream, conserving its laminar character.

This type of flow is somewhat analogous to that observed around a lifting airfoil, controlled by the rotation of the hinge of a flap [11].

/25

In all these basic tests, the flow was visualized in the symmetry plane for mounting between two walls. As a matter of fact, the flow becomes three-dimensional on blowing, and the jet of course perturbs the flow along the wall toward which it is pointed.

The reduction in separation and wake obtained above by means of blowing more clearly illustrates what happens naturally in three-dimensional flow under the effect of the cross currents which are set up behind the model (cylinder or re-entrant step: Figure 3) when it is sufficiently inclined.

In a plane stream, the same phenomenon can also be observed without a jet or cross current, but only during the initial motion which precedes the establishment of the steady state (Figure 4) [11].

#### Application to Airfoils

The wind-tunnel results of C.J. Dixon [1] for a thin unswept wing of aspect ratio  $\lambda = 4.4$  have been confirmed and supplemented by the visualizations made in the ONERA hydrodynamic tunnel on a similar wing of aspect ratio  $\lambda = 2$  (Figure 5).

In the two cases, the jet was emitted laterally from the step above the top face at about a quarter chord from the pointed leading edge of the model (Figure 5B).

Examination of the flow in the mid-span plane at  $20^\circ$  angle of attack confirms that the generalized separation observed without the jet (Figure 5A) is reduced to a bulb at the leading edge and the site of a vortex is made turbulent by the jet. Behind the jet, the flow re-attaches and maintains its laminar character. Furthermore, the displacement of the stagnation point upstream toward the lower face leads to a considerable increase in the circulation around the wing: see diagram 5D and Figure 5E.



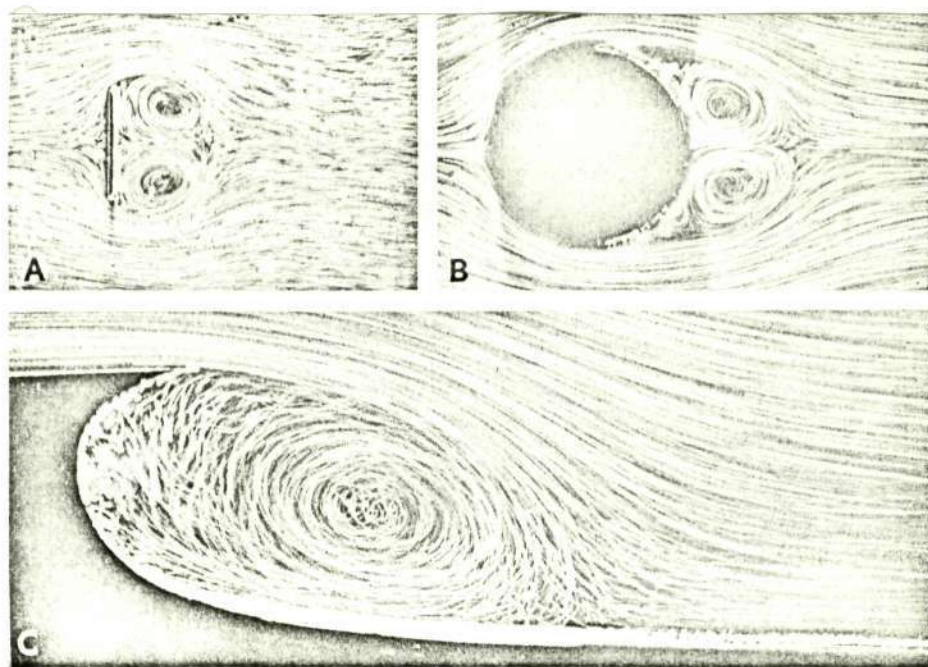


Figure 4. Flow around different "plane stream" models, during start-up.

- A Perpendicular plate ( $l = 40 \text{ mm} - i = 90^\circ$ ); B Cylinder ( $d = 50 \text{ mm}$ );  
C Stepped wall with point sloping toward the outside.

The plan view of the same phenomenon (Figure 5C) shows a slight incurving of the jet in the downstream direction by the external stream, as well as the limits of its effectiveness along the span (disruption of the edge vortex).

Figure 5F also shows that blowing moved nearer the leading edge gives a noticeable reduction in the separated bulb's size and a definite upstream displacement of the re-attachment point downstream from the jet.

Finally, Figures 5G and 5H reveal that the effectiveness of the jet extends to the highest angles of attack provided the intensity of the jet is sufficient.

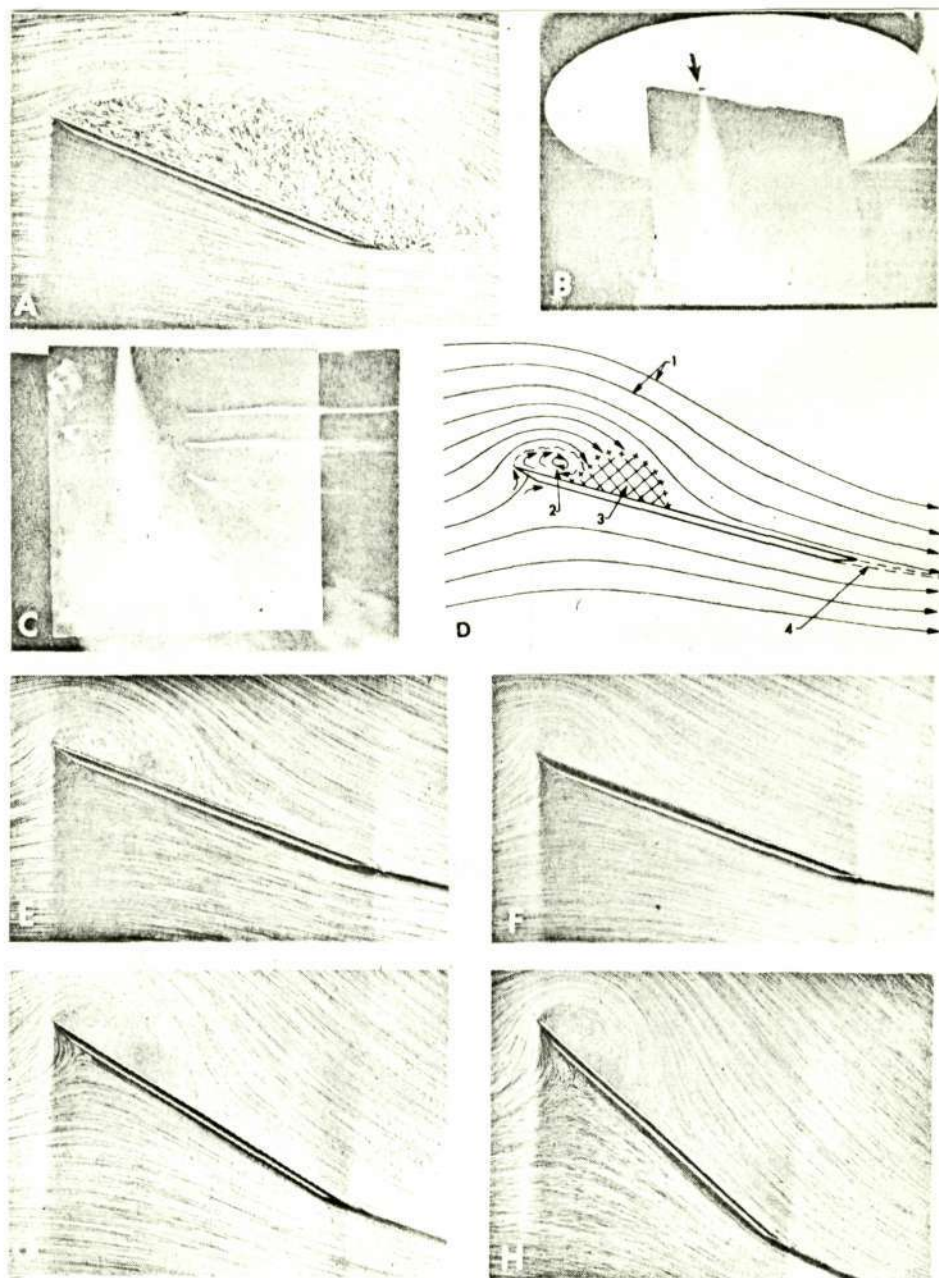


Figure 5. Lateral blowing on an unswept wing of low aspect ratio.

- A Flow without jet  
 B Perspective view showing injector position  
 C Flow on upper surface (colored liquid)

$i = 20^\circ$  unless otherwise indicated  
 jet injected at  $\frac{1}{4} l$

$$l = 100 - Re_l \approx 10^4 - \lambda = 2$$

$e = 2$  — pointed edges

(Figure 5 continued)

D	Diagram of flow with jet (see legend)	<u>Legend of Diagram</u>
E	Flow with jet	1 Streamlines
F	Flow with jet injected at $\frac{1}{2} l$	2 Separated bulb at leading edge
G	Flow with jet, $30^\circ$ angle of attack	3 Cross jet (sectional view)
H	Flow with jet, $40^\circ$ angle of attack	4 Wake resulting from confluence of the two laminar boundary layers

Views A, E, F, G, and H represent mid-span sections visualized by air bubbles.

As an example, we see that re-attachment on the thin wing ( $\lambda = 2$ ) tested in the tunnel is observed at  $20^\circ$  angle of attack for a value of the momentum coefficient

$$C_\mu = \frac{QmV_i}{\frac{1}{2} \rho V_o^2 S_{\text{wing}}} \quad \text{equal to } 0.8.$$

Under the same conditions ( $i = 20^\circ$ ,  $C_\mu = 0.8$ ), Dixon obtained the maximum value for the lift coefficient,  $C_z \sim 2.6$ , of his model ( $\lambda = 4.4$ ) in the wind tunnel [1].

A second wing example is that of a trapezoidal airfoil tested simultaneously in the Cannes wind tunnel ( $\lambda = 6$ ) and in the Chatillon hydrodynamic tunnel ( $\lambda = 5$ ) (Figure 6).

The visualizations obtained indicate that the procedure maintains all its effectiveness for this wing with a classic section (NACA 0012). The measurements performed show a considerable increase in the limiting angle for separation, and an increase in lift obtained beyond the appearance of separation, thus confirming the results of C.J. Dixon [1]. /27

Figure 7 reviews a trial application to an aircraft model with a slightly swept wing equipped with a deflected flap (see diagram 7F).



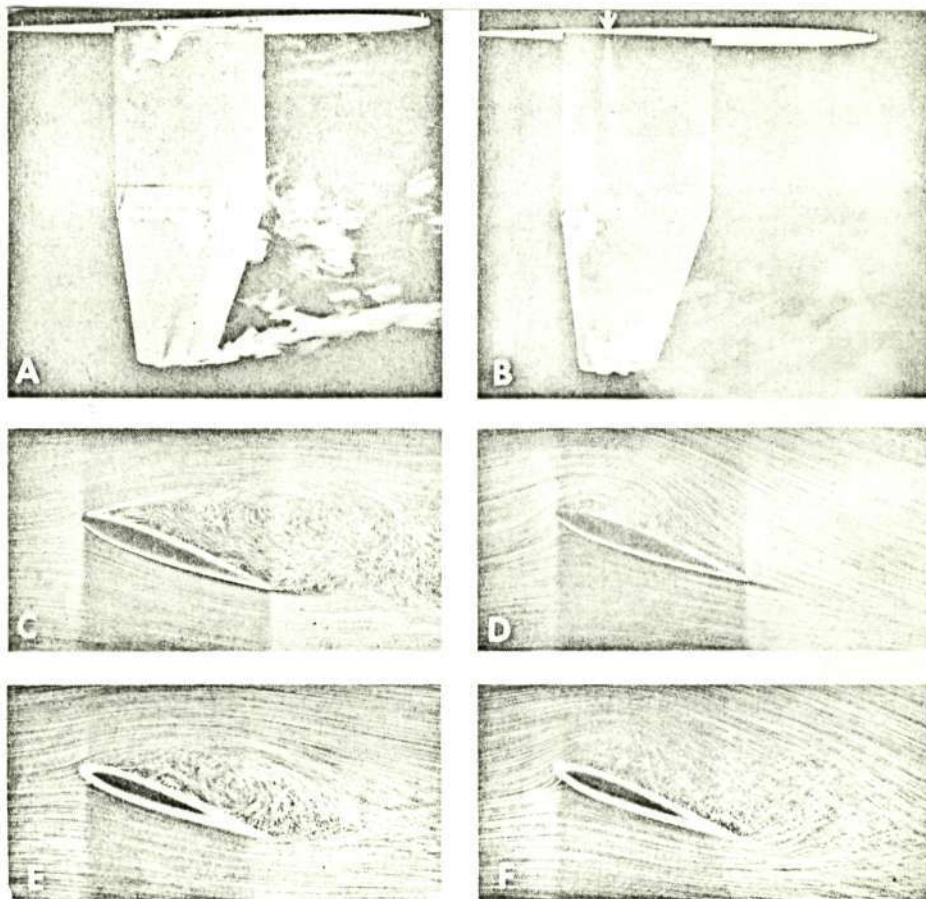


Figure 6. Lateral blowing on a trapezoidal wing of aspect ratio  $\lambda = 5$ .

- |   |                                |                                     |
|---|--------------------------------|-------------------------------------|
| A | Upper-surface flow without jet | } colored liquids                   |
| B | Upper-surface flow with jet    |                                     |
| C | Flow without jet               | } longitudinal sections at 1/3 span |
| D | Flow with jet                  |                                     |
| E | Flow without jet               | } longitudinal sections at 2/3 span |
| F | Flow with jet                  |                                     |

$i = 20^\circ$  — jet emitted at  $\frac{1}{4} l$

$l = 60$  —  $Re_1 \approx 0.6 \times 10^4$

NACA 0012 section

Note: re-attachment at 1/3 span occurs at  $i = 20^\circ$  for  $C_\mu \approx 0.25$ .

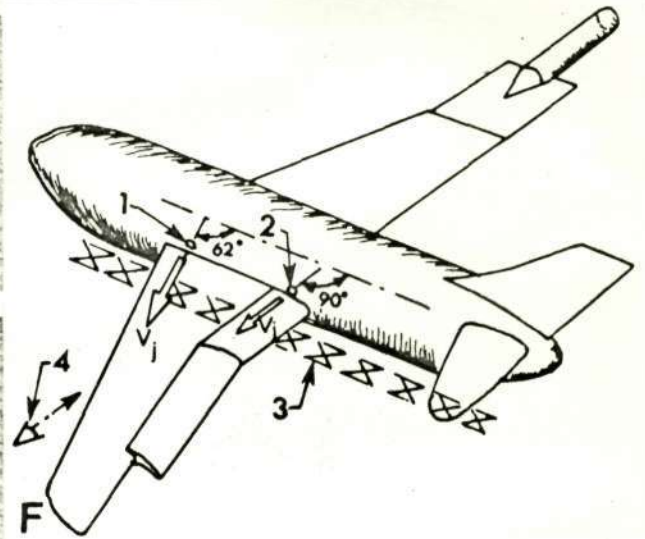
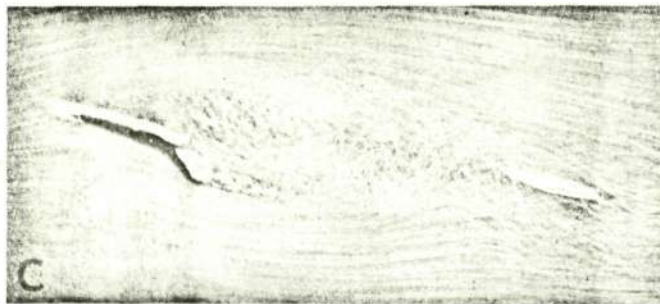
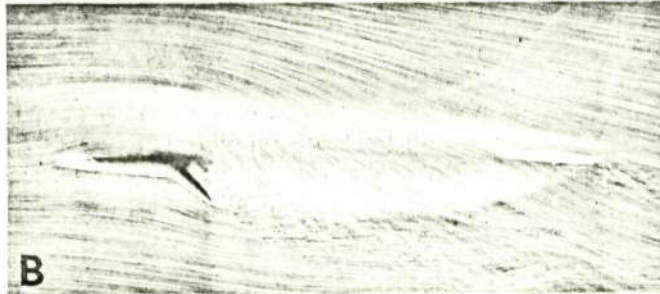


Figure 7. Lateral blowing on a weakly-swept wing on an aircraft model.

$$\phi_{BA} = 30^\circ, 5 - \frac{1}{m} = 26$$

$$Re_{1m} \sim 0.3 \times 10^4 - \text{flap set at } 25^\circ$$

- |   |                             |                   |
|---|-----------------------------|-------------------|
| A | Flow without jet            | } $i = 2.5^\circ$ |
| B | Flow with flap jet          |                   |
| C | Flow without jet            | } $i = 10^\circ$  |
| D | Flow with moderate wing jet |                   |
| E | Flow with intense wing jet  |                   |
| F | Diagram of model            |                   |

1 jet injected at  $\frac{1}{4}$  of the wing

2 jet injected at  $\frac{1}{4}$  of the flap

3 section of flow visualized

4 axis of photographs

Visualizations made in the plane where the engine is located show the usefulness of the procedure:

- on the one hand, at low angles of attack, when it is applied to the flap only (jet issuing near the hinge of the flap: Figures 7A and 7B);
- on the other hand, at high angles of attack, when it extends over the whole wing (jet emerging near the leading edge: Figures 7C, 7D, and 7E).

Finally, Figure 8 recalls the first attempt to retard, with the aid of a jet, the bursting of the vortices of a delta wing at high angles of attack (Figures 8A and 8B).

It also illustrates a more elaborate and more recent application of the method: the turbulent jet emerges at mid-chord downstream from the bursting point, and is directed along the axis of the vortex. It not only delays the appearance of the bursting point and straightens out the vortex, but also causes the vortex to curve inward toward the after point by considerably extending the central sound, non-turbulent part of the flow at the expense of the eddy zone which usually forms at the after point. /31

Similar experiments with the Cannes wind tunnel on a  $45^\circ$  delta wing have confirmed that the major effects of the blowing were an increase in lift ( $\Delta C_z \sim 2 \text{ to } 6 C_{\mu}$ ), and a decrease or suppression of the tendency to nose-up at high angles of attack. Thus, at  $25^\circ$  angle of attack,  $C_z$  is found to be 1.6 with a jet emerging at the quarter chord and characterized by  $C_{\mu} \sim 0.1$  [6].

#### Application to Diffusers

The properties of lateral blowing have been applied to diffusers which have a large vertex angle ( $2\alpha = 30^\circ$ ). As for the wings, tests were undertaken simultaneously in the wind tunnel and hydrodynamic tunnel. This study first used two-dimensional models with injectors in the side wall at the step located at the end of the parallel upstream channel (see Diagram 11 A).



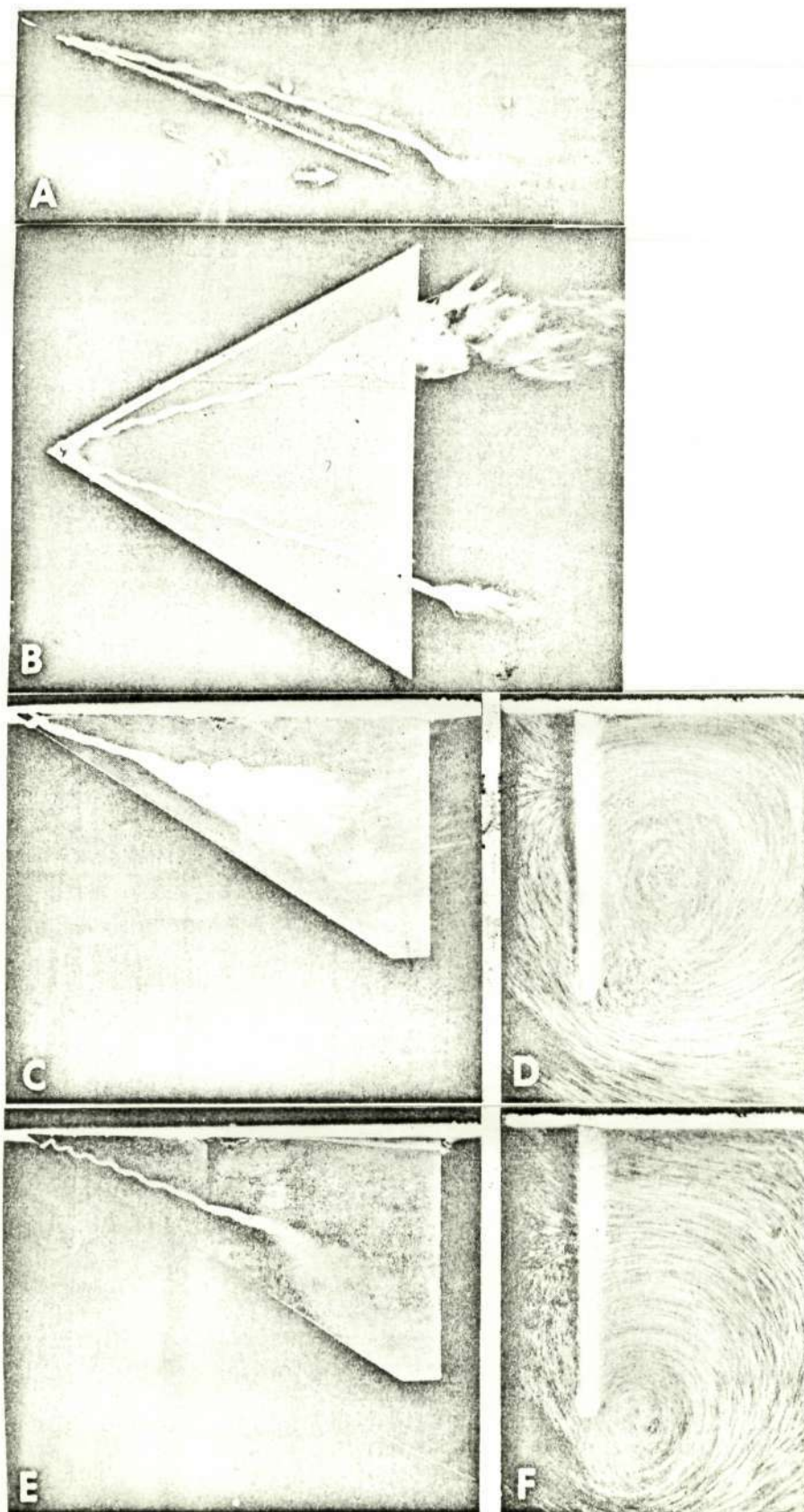


Figure 8. Caption on following page.

Figure 8 (continued). Flow around a thin delta wing with pointed edges at non-zero angle of attack in the presence of a jet emitted along the axis of the apex vortex.

A Profile view	}	entire model $I = 100 - Re_I \approx 5 \times 10^3$ $I = 20^\circ - \varphi_{BA} = 60^\circ$
B View of upper surface		with jet injected from lower surface in direction of left vortex
C View of upper surface without jet (and no injector)	}	semi-model fixed to the wall:
D Transverse section near trailing edge, without jet		$I = 25^\circ - I = 150 -$ $\approx 1,5 \times 10^4 \varphi_{BA} = 60^\circ$
E View of upper surface with jet		— jet injected at mid-chord exactly along the axis of the vortex;
F Transverse section near trailing edge, with jet		$C_{\mu} = 0.5.$

Visualization by colored liquid injected into the axis of the vortices (views A, B, C, and E).

For a simple diffuser (Figures 9A to 9D), the flow emerging from the upstream channel separates in the diffuser when there is no jet. Under the conditions of the hydrodynamic tunnel ( $Re_H \approx 3 \times 10^4$ ), the stream curves toward one or the other of the walls, thus becoming asymmetric (Figure 9A). A cross jet can tilt the flow toward the wall on which the blowing takes place (Figure 9B); the curvature of the flow remains after the jet is stopped (Figure 9C). With this model, it was not possible to obtain correct re-attachment on both sides by means of double injection without making the axial flow split in two, since the two jets expand on the side wall toward which they are pointed, then reunite in the center of the model (Figure 9D). It is likely that an improvement could be made if the shape were completed, as in Figure 1, by two partial ducts associated with the two jets. /32

In contrast, the wind-tunnel experiment is more conclusive (Figure 11B): double injection provides complete re-attachment, while single injection

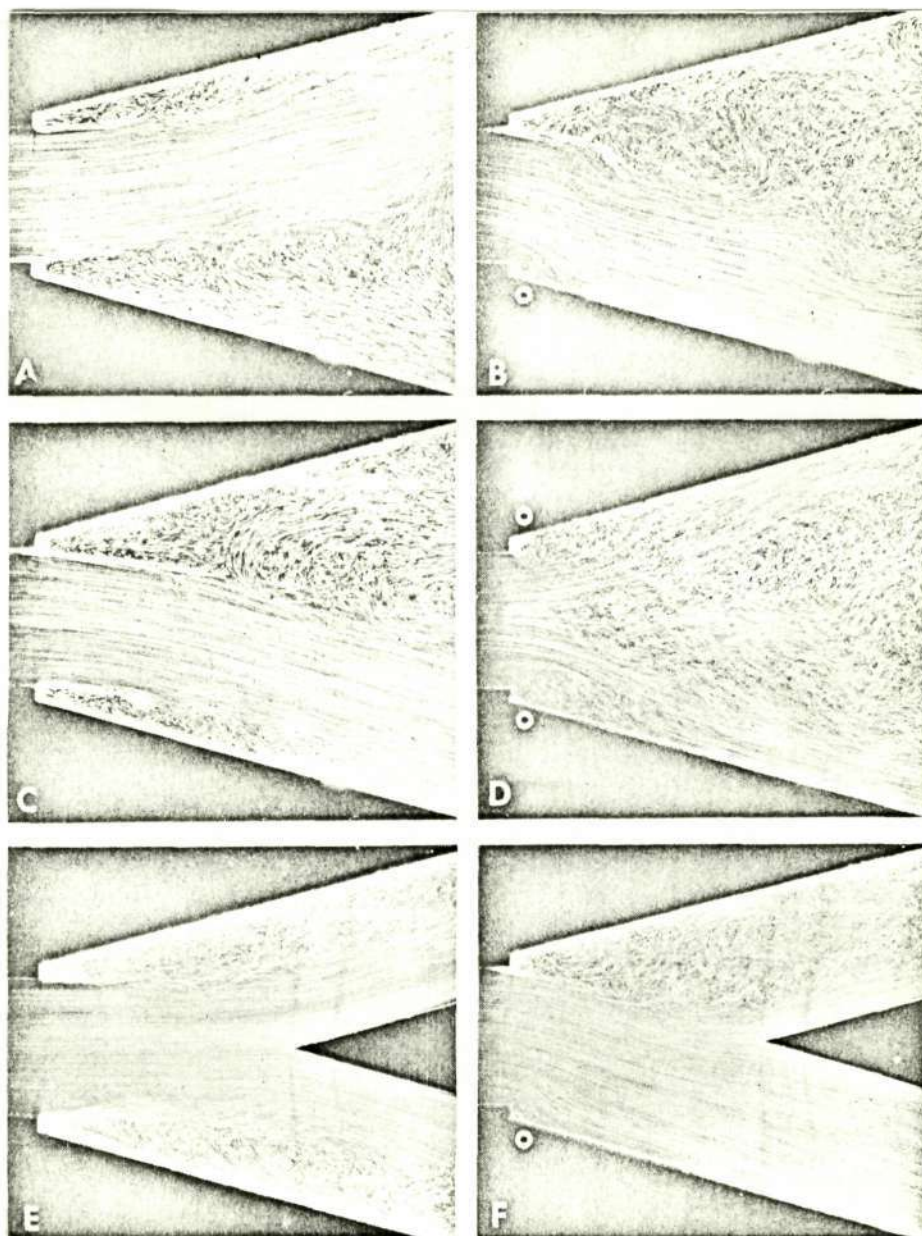


Figure 9. Flow in the symmetry plane of a large-diameter, two-dimensional diffuser with lateral blowing.

- A Test without jet ( $C_\mu = 0$ )
- B Test with lower cross jet ( $C_\mu = 0.2$ )
- C Test without jet after stopping preceding jet ( $C_\mu = 0$ )
- D Test with upper and lower cross jets ( $C_\mu = 0.4$ )

(Caption continued on following page)

Figure 9 (continued)

E Test without jet ( $C_\mu = 0$ )	}	model modified into a two-duct fluid system
F Test with lower cross jet ( $C_\mu = 0.2$ )		

$$\left. \begin{array}{l} 2\alpha = 30^\circ \\ H = 60 \\ Re_H \approx 300^4 \end{array} \right|$$

(See Figure 11A)

channels the principal flux in the blowing direction. In the absence of the jet, the separated stream maintains an axial position.

Based on these tests, the application to fluidics can be considered.

The utility of the procedure for a two-duct system is confirmed by Figures 9E and 9F. The axial dihedron inserted to produce the two ducts has the effect of restoring and stabilizing the separated stream in its axial position when the blowing stops.

Figure 10 illustrates the case of a three duct system, for which the two dihedra which are inserted do not have the same effect.

The experiment shows that a lateral jet of short duration tilts the stream into one or the other of the extreme ducts located on the blowing side; the position acquired is maintained after the jet stops (Figures 10A to 10C). The axial position observed at the start of the test (Figure 10D) probably can be resumed only by means of a cross jet in the symmetry plane.

Finally, this study is presently being carried out for an axi-symmetric diffuser of the same diameter; the lateral blowing is produced by four injectors located every  $90^\circ$ , with the same rotational direction.



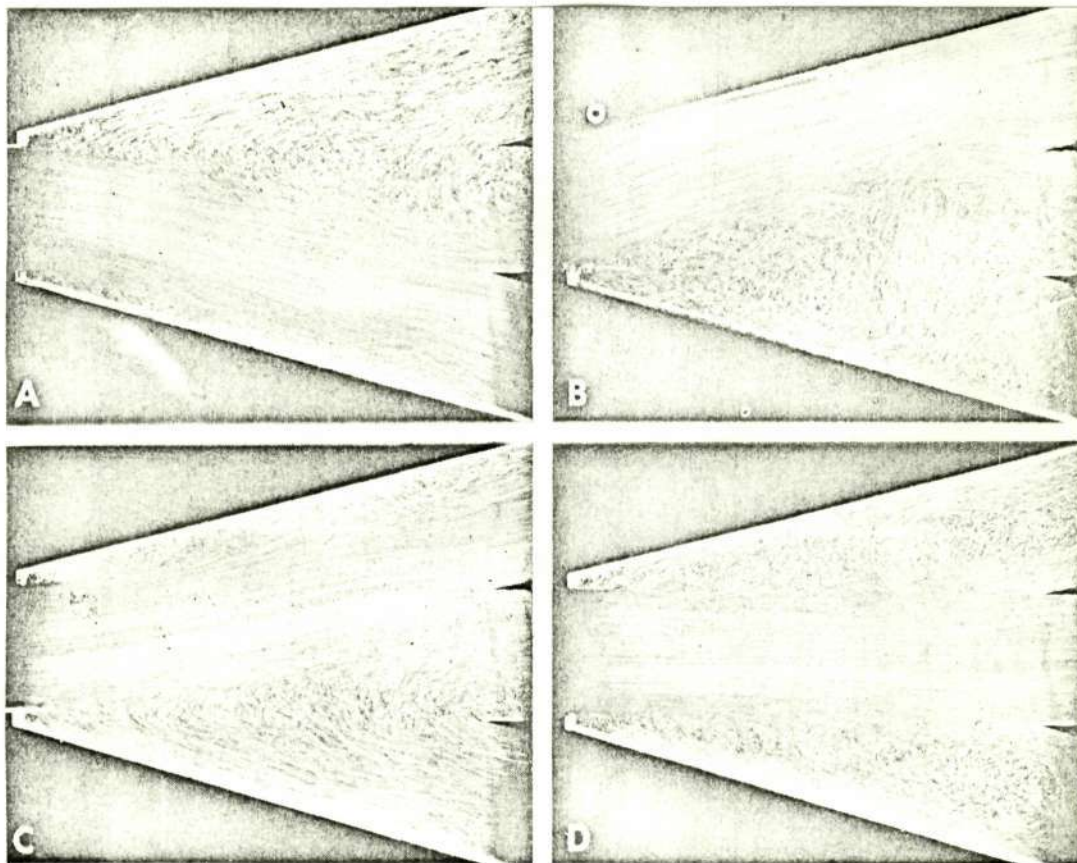


Figure 10. Flow in the symmetry plane of a large-diameter, two-dimensional diffuser, with lateral blowing.

- A Test without jet after stopping lower jet ( $C_\mu = 0$ )
- B Test with upper cross jet ( $C_\mu = 0.2$ )
- C Test without jet after stopping preceding jet ( $C_\mu = 0$ )
- D Test without jet just after start of test ( $C_\mu = 0$ )

Model modified into three-duct fluidic system

$$2\alpha = 30^\circ - H = 60$$

$$Re_H \approx 3 \times 10^4$$

(See Figure 11A)

The visualizations obtained during the developmental tests showed that blowing of sufficient intensity allows one to obtain effectively complete

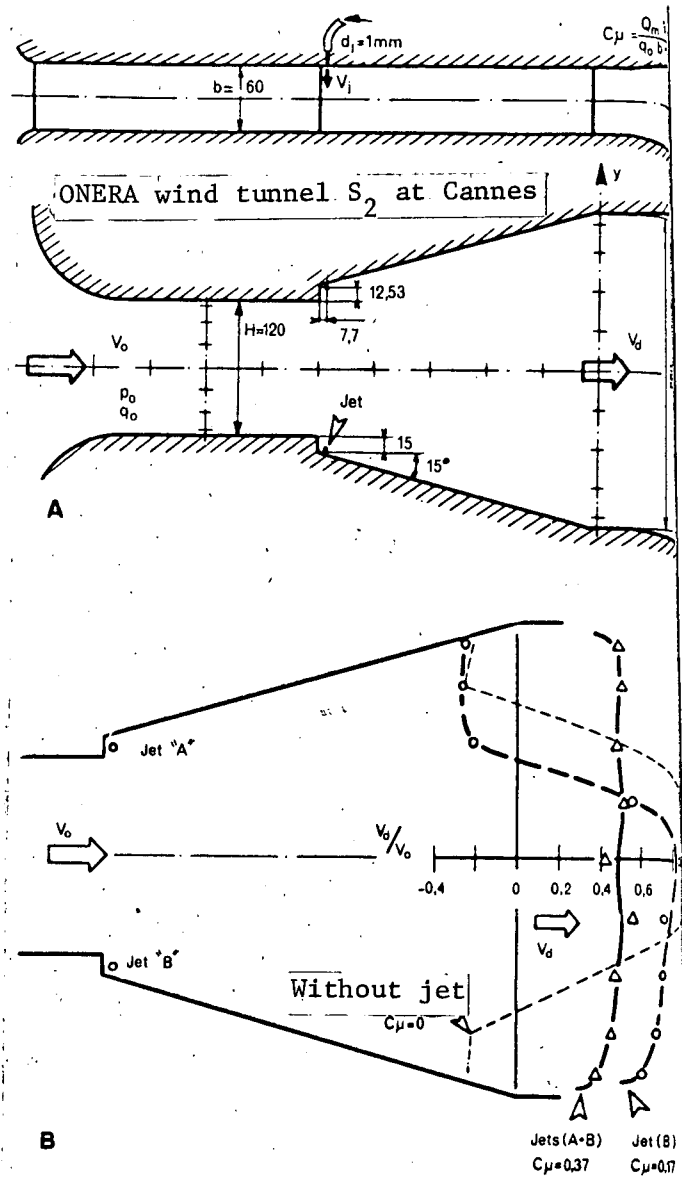
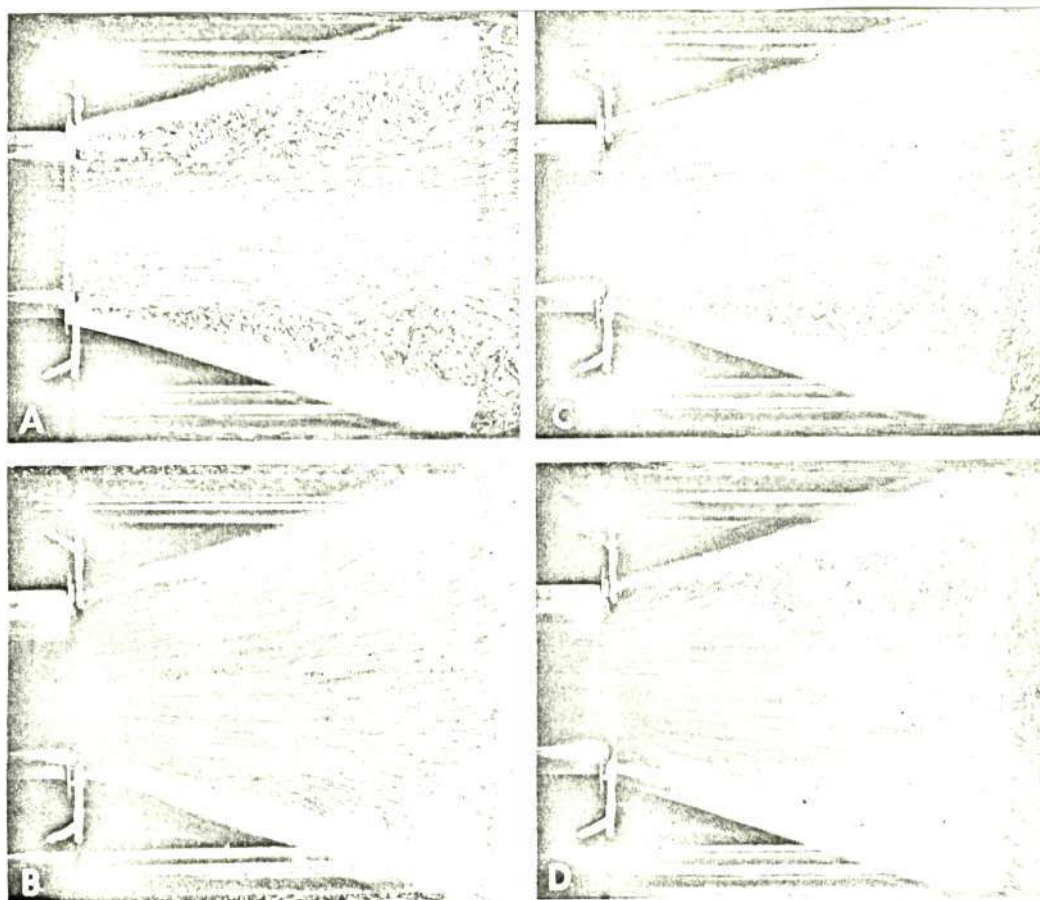


Figure 11. Test in the ONERA S<sub>2</sub> wind tunnel at Cannes of a large-diameter two dimensional diffuser model, with lateral blowing.

- A Diagram of the model (about twice the size of the model ( $H=60$ ) tested in the hydrodynamic tunnel, except for the breadth  $b=60$ , which is unchanged)
- B Velocity distribution at diffuser outlet obtained during testing for  $C_\mu = 0$  (test without jet)
- $C_\mu = 0.17$  (test with a single jet)
- and  $C_\mu = 0.37$  (test with two jets)

$$Re_H \approx 10^5$$





Reproduced from  
best available copy.

Figure 12. Flow in diametral plane of large-diameter axisymmetric diffuser, with lateral blowing.

A Test without jet

$2\alpha = 30^\circ - d = 60 - Re_d \approx 1,5 \cdot 10^4$  Blowing

B Test with intense jets

by four jets arranged every  $90^\circ$

C } Tests with less intense jets  
D }

re-attachment on the diffuser (Figures 12A and 12B), while at a reduced intensity the flow acquires an accentuated, unsteady character with the stream separating and re-attaching successively on different sections of the model (Figures 12C and 12D).

### Conclusion

This study confirms all the advantages of a cross jet as the original suggestion for flow control.

It shows both the good agreement between wind-tunnel and hydrodynamic-tunnel results for high-lift wings, and promising flows for application to diffusers and fluidic systems.

However, tests carried out in each case, and under real conditions, must still determine the energy balance of this type of flow control.

### REFERENCES

1. Dixon, C.J. Lift Augmentation by lateral Blowing over a Lifting Surface. AIAA Paper No. 69-193, AHS VTOL Research Design and Operations Meeting.
2. Werlé, H. Division and Coming Together of Fluid Flows. Rech.Aéron. No. 79, 1960.
3. Roy, M. Formation of Turbulent Zones in Low-Viscosity Flows. 3rd Ludwig Prandtl Conference, Z. Flugw. No. 8 (8/59), published by ONERA.
4. Werlé, H. Bursting Phenomena of Vortices at the Apex of a Delta Wing at Low Velocities. Rech.Aéron. No. 74, 1960.
5. Cornish, J.J., III. High Lift Applications of Spanwise Blowing. ICAS Paper No. 70-09, 7th Congress, Rome, September 1970.
6. Poisson-Quinton, Ph. Contrôle du décollement d'une surface portante par un jet transversal (Control of Separation on a Lifting Surface by a Cross Jet). Paper presented at ICAS Congress, Rome, September, 1970.
7. ONERA Film 649. Contrôle de l'écoulement par soufflage latéral (Flow Control by Lateral Blowing), 1971, 16mm, 10 min.
8. L'Aéronautique et l'Astronautique, No. 22, 1970-6, cover and p. 1.
9. Werle, H. Aperçu sur les possibilités expérimentales du tunnel hydrodynamique à visualisation (Summary of the Experimental Capabilities of the Hydrodynamic Tunnel with Visualization), ONERA Technical Report No. 48, 1958.

10. Werlé, H. Methods of visualizing hydraulic flows. La houille blanche No. 5, 1963.
11. Werlé, H. Visualisation hydrodynamique des écoulements instationnaires (Hydrodynamic Visualization of Transient Flows). ONERA Technical Report No. 180, 1971.

Translated for National Aeronautics and Space Administration under contract No. NASw 2035, by SCITRAN, P. O. Box 5456, Santa Barbara, California 93108